Dietary Genistein Inhibits Metastasis of Human Prostate Cancer in Mice

Minalini Lakshman,[1] Li Xu,[1] Vijayalakshmi Ananthanarayanan,[2] Joshua Cooper,[4] Chris H. Takimoto,[4] Irene Helenowski,[2] Jill C. Pelling,[3] and Raymond C. Bergan[1]

[1]Division of Hematology/Oncology, Department of Medicine, [2]Department of Preventive Medicine, and [3]Department of Pathology, Northwestern University Medical School and Robert H. Lurie Cancer Center of Northwestern University, Chicago, Illinois and [4]Institute for Drug Development, San Antonio, Texas

Abstract

Dietary genistein has been linked to lower prostate cancer (PCa) mortality. Metastasis is the ultimate cause of death from PCa. Cell detachment and invasion represent early steps in the metastatic cascade. We had shown that genistein inhibits PCa cell detachment and cell invasion *in vitro*. Genistein-mediated inhibition of activation of focal adhesion kinase (FAK) and of the p38 mitogen-activated protein kinase (MAPK)–heat shock protein 27 (HSP27) pathway has been shown by us to regulate PCa cell detachment and invasion effects, respectively. To evaluate the antimetastatic potential of genistein, we developed an animal model suited to evaluating antimetastatic drug efficacy. Orthotopically implanted human PC3-M PCa cells formed lung micrometastasis by 4 weeks in >80% of inbred athymic mice. Feeding mice dietary genistein before implantation led to blood concentrations similar to those measured in genistein-consuming men. Genistein decreased metastases by 96%, induced nuclear morphometric changes in PC3-M cells indicative of increased adhesion (i.e., decreased detachment) but did not alter tumor growth. Genistein increased tumor levels of FAK, p38 MAPK, and HSP27 "promotility" proteins. However, the ratio of phosphorylated to total protein trended downward, indicating a failure to increase relative amounts of activated protein. This study describes a murine model of human PCa metastasis well suited for testing antimetastatic drugs. It shows for the first time that dietary concentrations of genistein can inhibit PCa cell metastasis. Increases in promotility proteins support the notion of cellular compensatory responses to antimotility effects induced by therapy. Studies of antimetastatic efficacy in man are warranted and are under way. [Cancer Res 2008;68(6):2024–32]

Introduction

Prostate cancer (PCa) is the second most common cause of cancer-related death in American men (1). Death is caused by the formation of PCa metastases (2). Therapy that could prevent the formation of metastases would thus have the potential for high clinical effect. There is currently no effective means to inhibit PCa metastasis.

Cell detachment and cell invasion represent initial steps in the metastatic cascade (3–5). The putative PCa chemopreventive drug genistein was initially shown by us to inhibit human PCa cell detachment (6, 7) and then invasion (8, 9). Cell detachment was inhibited in a time-dependent and concentration-dependent manner in several human PCa cell lines (6). Focal adhesion kinase (FAK) mediates cell adhesion-associated signals in many cell types (10–12) and was shown by us to do so in human PCa (7). FAK is up-regulated during PCa progression, particularly in metastatic cells (13, 14). Genistein was shown by us to inhibit FAK phosphorylation (i.e., activation) in human PCa cells (15).

Through a series of related investigations, we have identified several signaling pathways which cooperate to regulate PCa cell invasion and have shown that genistein inhibits proinvasion signaling through them (8, 9, 16–20). Our findings suggest that p38 mitogen-activated protein kinase (MAPK) seems to be particularly important. Specifically, p38 MAPK was necessary for phosphorylation of heat shock protein 27 (HSP27), which in turn was necessary for matrix metalloproteinase type 2 (matrix metalloproteinase (MMP)-2) activation, and PCa cell invasion (8, 16). HSP27 is up regulated during PCa progression, particularly in metastatic cells (16, 21–23). Genistein inhibits HSP27 phosphorylation, MMP-2 induction, and cell invasion, by blocking phosphorylation (i.e., activation) of p38 MAPK (8, 9). p38 MAPK is also important because we have shown that it can activate Smad3 through signaling pathway cross-talk (17). We then showed that Smad3 increased human PCa cell invasion and that genistein could abrogate its proinvasion action (19, 20). Together, these studies suggest that genistein inhibits initial steps in the metastatic cascade of human PCa and indicate that inhibition of activation of FAK and of the p38 MAPK-HSP27 pathway may be important.

Genistein is found in soy, and soy consumers have blood concentrations ∼2 logs higher than nonsoy (i.e., red meat) consumers (24, 25). Rates of PCa mortality (and thus metastasis) correlate inversely with blood concentrations of genistein (26–28). Soy-consuming Southeast Asians have PCa mortality rates ∼10-fold lower than nonsoy-consuming Westerners but approach Western rates after migration. Some studies suggest that the prevalence of organ confined PCa (i.e., primary PCa) may be similar (i.e., 2-fold lower or equal) across cultures (27, 29). If genistein were inhibiting metastasis, one would expect to find the above observations.

In the current study, dietary genistein is shown to inhibit human PCa metastasis. Evidence is provided that this is associated with inhibition of PCa cell detachment *in vivo*. While FAK, p38 MAPK, and HSP27 proteins increased in response to treatment, genistein effectively blocked their activation.

Materials and Methods

Preparation of green fluorescent protein–PC3-M cells. The origin and culture conditions for PC3-M human PCa cells have been described (13). green fluorescent protein (GFP)–PC3-M cells were engineered by selecting cells transfected with GFP under G418 growth conditions, as described (18). For implantation, cells were suspended in 35 μL of RPMI 1640 (Life Technologies). For sham mice, no cells were added.

Animals and diet formulation. Four-week-old inbred male athymic BALB/C mice from Charles River Laboratories were treated under a Northwestern University IACUC–approved protocol, housed in a barrier facility with 12-h light/dark cycles, and given food and water *ad libitum*. One week before implantation, mice were fed soy-free Harlan Teklad 2016S chow, to which 0, 100, or 250 mg genistein (ICN)/kg chow were added.

Orthotopic implantation of PCa cells. The prostate was delivered through a lower abdomen midline incision, and the dorsal lobes were exposed. Cells were injected under the capsule of the right lobe through a 30-gauge needle, thus forming a bleb that remained intact after needle withdrawal. Using blue dye, separate studies confirmed this adequacy of technique (data not shown). The peritoneum was closed with 4 to 0 polyvinyl, and the skin was stapled.

Gross and histologic examination of organs. All major organs, including brain and bone (femur and pelvic), and resulting body cavities were grossly examined for metastasis. Organs were weighed and fixed in 10% formalin (bone was first decalcified). A portion of tissue samples were snap frozen. From measures taken in two perpendicular dimensions, tumor volume was calculated as $0.52 \times (\text{width})^2 \times (\text{length})$.

All major organs were examined for microscopic evidence of metastasis. Step sections of 1 to 3 mm were performed on formalin-fixed paraffin-embedded tissue, and 5 μm cuts were stained with H&E, as described (30). Lungs were step sectioned in the sagittal plane in 30-μm cuts, followed by 5-μm cuts for H&E staining. All necropsies and tissue analysis were performed by a single person (M.L.). H&E confirmation of metastasis was required to score an organ as positive for metastasis.

Measurement of plasma genistein concentration. From blood collected via cardiac puncture, as described (31), total plasma genistein was measured as described, with modifications (32). Briefly, 100 μL of 50,000 ng/mL 4-hydroxybenzophenone in *tert*-butyl methyl ether were added to 0.1 mL of plasma extracted with 3 mL of *tert*-butyl methyl ether, the resultant organic layer was evaporated to dryness, and samples were redissolved in 80:20 (v/v) 0.05 mol/L ammonium formate (pH 4.0)/methanol. Separation was performed on a Waters Alliance high-pressure liquid chromatography system, using a Nova-Pak C8 3.9×150 mm reverse-phase analytic column and a Nova-Pak C8 guard column (Waters Corp.). Using a gradient mobile phase and a Waters 996 diode array UV detector, total genistein standards were linear over 65 to 10,000 ng/mL, and assay-to-assay and day-to-day variability was below 10%. Values below the lower limit of quantitation (LLQ) were estimated as the mean of 0 and LLQ.

Immunohistochemistry. Tissues were stained for GFP expression, as previously described, with modifications (33). In the current study, anti-GFP antibody (clone A11122, Molecular Probes) was diluted 1:50 in 5% goat serum and signal detected with the EnVision + System (DAKO). Positive (GFP-PC3-M cells) and negative (antibody isotype) controls were always included.

Quantitative image analysis. For *in vitro* studies, PC3-M cells were stained with rhodamine-phalloidinn and 4′,6-diamidino-2-phenylindole (DAPI) to visualize filamentous actin (i.e., the whole cell) and cell nuclei, respectively, as previously described (15, 18). Cells were imaged on a Zeiss Axioskop Microscope, and cell and nuclear morphology of actin and DAPI images, respectively, determined with MetaMorph V6.0 software (Molecular Devices, Inc.). For each time and genistein concentration treatment condition, ≥10 cells or nuclei were evaluated.

In vivo analysis of nuclear morphology was performed as described, with modifications, on formalin-fixed paraffin-embedded primary tumor and metastatic lymph node tissue (34). Briefly, the nuclei of 7-μm tissue sections were stained with Feulgen using an established protocol (35) and then scanned on an ACIS II Quantitative Image Analysis Workstation (Clarient, Inc.) using the Tissue Ploidy software protocol. From regions prospectively identified on adjacent H&E-stained sections, images of individual nuclei extracted by the ACIS system are presented for "acceptance" or "rejection" by the operator. Reasons for rejection include overlapping nuclei or nuclei from nonepithelial cells. We modified the program algorithm to include nuclei of varying sizes, thus providing a "wide" filter setting so as to avoid potential bias by sampling only larger cells. Morphometric variables of accepted nuclei are determined by preset program algorithms and exported into MS Excel files for further analysis. For each tissue type (i.e., primary tumor or lymph node metastasis), within a given diet group (i.e., control or genistein treated), ≥500 nuclei were evaluated (using tissue from five different mice). All tissue was processed and evaluated at the same time, in a blinded fashion, by a single person (V.A.).

Western blots. Protein isolation from tissue was performed as described, with modifications (36–38). Briefly, snap frozen tumor tissue was extracted with radioimmunoprecipitation assay buffer containing protease (aprotinin, leupeptin, pepstatin, and 1 mmol/L EDTA) and phosphatase inhibitors (NaVO₄, NaF, and phosphatase inhibitor cocktails 1 and 2; Sigma). Immunoblotting for phosphorylated and total FAK (7), p38 MAPK (8), and HSP27 (16) were performed as described.

Statistical analysis. When more than one treatment group was compared, differences were compared by means of one-way ANOVA. The difference between two groups was compared using a two-sided t test. In some instances, as indicated, prior experiments have shown us one direction in which the change would be occurring, and therefore, we used a one-sided t test. Differences were considered statistically significant for P values of ≤0.05. The Spearman correlation coefficient was used to evaluate the association between tumor weight and metastatic burden. Statistical tests were performed with the statistical software package (SAS, V9.1).

Results

Growth and metastasis of PCa cells after orthotopic implantation. The design of all animal experiments is outlined in Supplementary Fig. S1. The extent and timing of metastatic spread after orthotopic implantation of GFP-PC3-M cells was first characterized. In study 1, cohorts of 10 mice in total for each time point were implanted with 10^6 cells, and necropsy was performed after 2, 3, or 4 weeks. The combined findings from two separate identical experiments, performed at different times, involving a total of 29 mice (one mouse died shortly after surgery), are compiled in Supplementary Table S1*A*. At 2 weeks, microscopic primary tumors were evident in 100% of mice. Macroscopic tumors were seen at 3 weeks but did not increase further at 4 weeks (Fig. 1*A*). Tumor volume ranged from 0.52 to 3.12 cm³. By 3 weeks, pathologically enlarged periaortic, periadrenal, and axillary lymph nodes were found in 100%, 40%, and 0% of mice, respectively. In all instances, the presence of tumor was confirmed by histologic examination. Microscopic examination of major organs found metastases in the lung in 70% of mice, whereas no metastases were detected in any other organs. By 4 weeks, metastases to periadrenal lymph nodes and lung had increased to 32% and 84%, respectively. No metastases were detected in liver, bone marrow, kidney, brain, or axillary lymph nodes. Figure 1*B* depicts representative histologic findings of cancer cells in periaortic and periadrenal lymph nodes.

The affect of surgery and tumor growth, upon food intake and body weight, were evaluated next. In this experiment, five mice were sham-injected and five mice were implanted with 10^6 GFP-PC3-M cells at the same time. This was repeated at a separate time, giving 10 mice per cohort. Weekly food consumption was relatively constant over the 4-week time course and was similar across cohorts (Supplementary Fig. S2). Both cohorts were gaining weight at 2 weeks, and this trend continued for sham mice (Fig. 1*C*). After 2 weeks, the implant cohort lost weight, and by 4 weeks, this was

>10% of presurgery weight. Future experiments did not exceed 4 weeks.

Study 2 examined the effect of cell number on metastatic spread. Mice, in cohorts of 7, were implanted with 10^4, 10^5, or 10^6 GFP-PC3-M cells. Findings from necropsy performed at 4 weeks are in Supplementary Table S1*B*. Macroscopic lymph node metastases and prostate tumors were found in 100% of mice in all groups. The average weight of prostate tumors was comparable across cohorts. Lung metastases were detected in 28%, 42%, and 100% of mice implanted with 10^4, 10^5, and 10^6 cells, respectively. To evaluate whether increased tumor size led to increased metastases, tumor volume and number of lung metastases were compared for each mouse. There was no correlation.

Characterization of lung metastases. A model wherein metastases can be readily quantified, but do not saturate the destination organ (in this case, lung), is well suited for evaluating antimetastatic drugs. Therefore, the current model was further characterized. Lung metastases were not associated with detect-able surface nodules in any mouse or with an alteration of lung weight (Fig. 1*D*). The abnormally large nuclei characteristic of GFP-PC3-M cells were readily visible on H&E-stained tissue, thus allowing easy detection (Fig. 1*D*). Detection of GFP by immuno-histochemistry definitively identified them as GFP-PC3-M cells (Fig. 1*D*). Staining for GFP did not detect additional GFP-PC3-M cells when compared with histomorphometric-based methods (data not shown).

As quantitative PCR (qPCR) using GFP-specific primers offered the potential for easy quantitation of GFP-PC3-M cells within mouse lung, a series of extensive experiments was performed to evaluate the potential utility of this approach, Supplementary Fig. 3. These experiments indicate that use of qPCR does not provide an accurate means of quantitating metastatic cells to the lung in the current model. Thus, further quantitation of lung metastasis was performed histomorphometrically.

Genistein inhibits PCa metastasis. In study 3, the ability of genistein to inhibit PCa metastasis was evaluated. Mice were
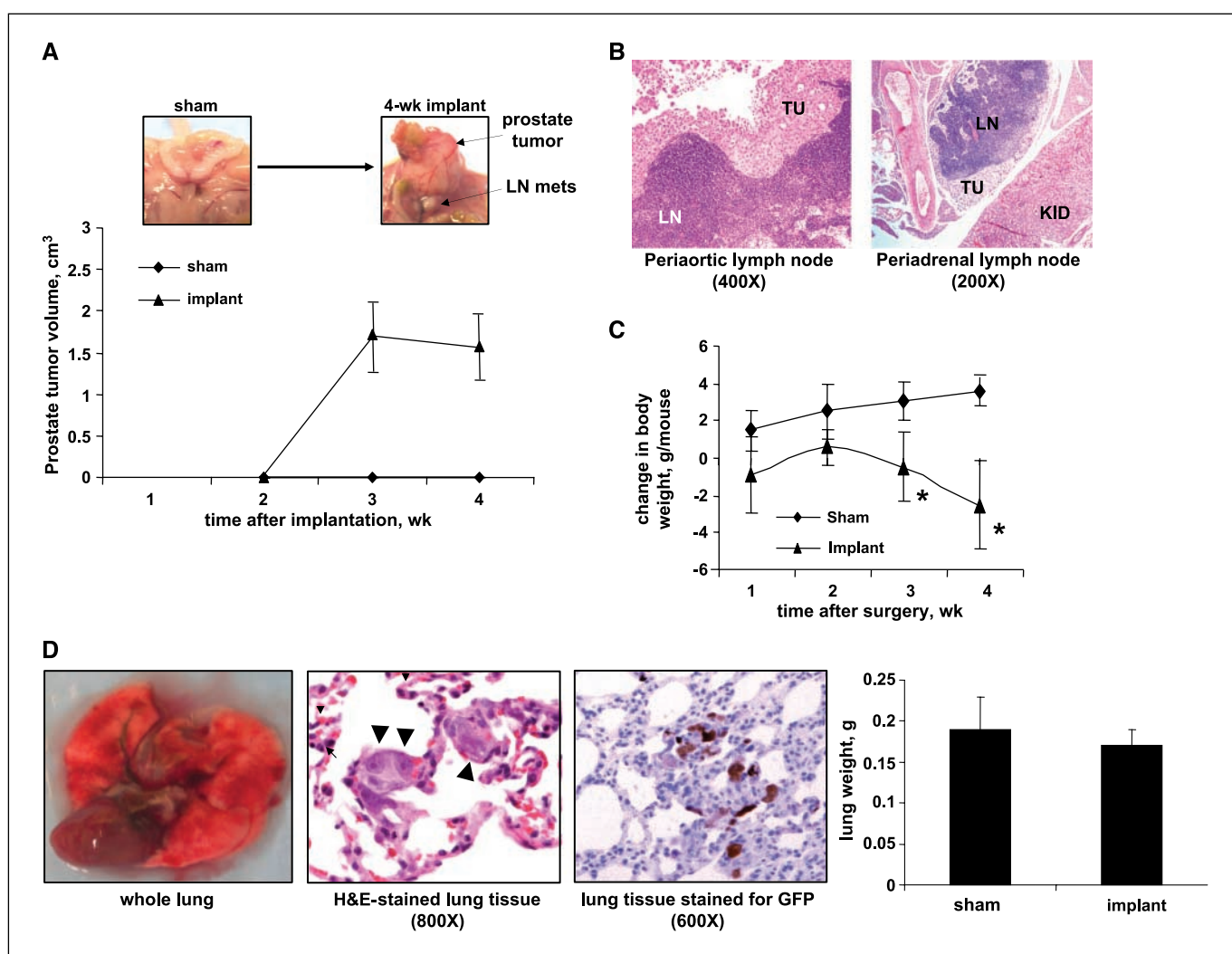
Figure 1. Growth and spread of PCa cells after orthotopic implantation into athymic mice. Mice were orthotopically implanted with 10^6 GFP-PC3-M cells (or sham), and necropsy was performed at 2, 3, or 4 wk. *A,* growth of prostate tumor. *Points,* mean volume of tumor in the prostate gland (n = 10 mice per time point); *bars,* SE. *B,* representative photomicrographs of periaortic and periadrenal lymph nodes; lymph node (*LN*), tumor (*TU*), and kidney (*KID*) are denoted. *C,* the effect of tumor growth on body weight. *Points,* mean body weight for 10 implanted and 10 sham mice; *bars,* SD. *,* differences between implanted and sham mice for $P \leq 0.05$ (two-sided *t* test). *D,* characterization of lung metastasis. Whole heart-lung organs resected *en block,* H&E-stained lung tissue (*black arrows,* GFP-PC3-M cells), and lung tissue stained for GFP. *Columns,* mean weight of lungs from mice 4 wk after implantation of 10^6 cells (n = 21) or sham (n = 7); *bars,* SE.
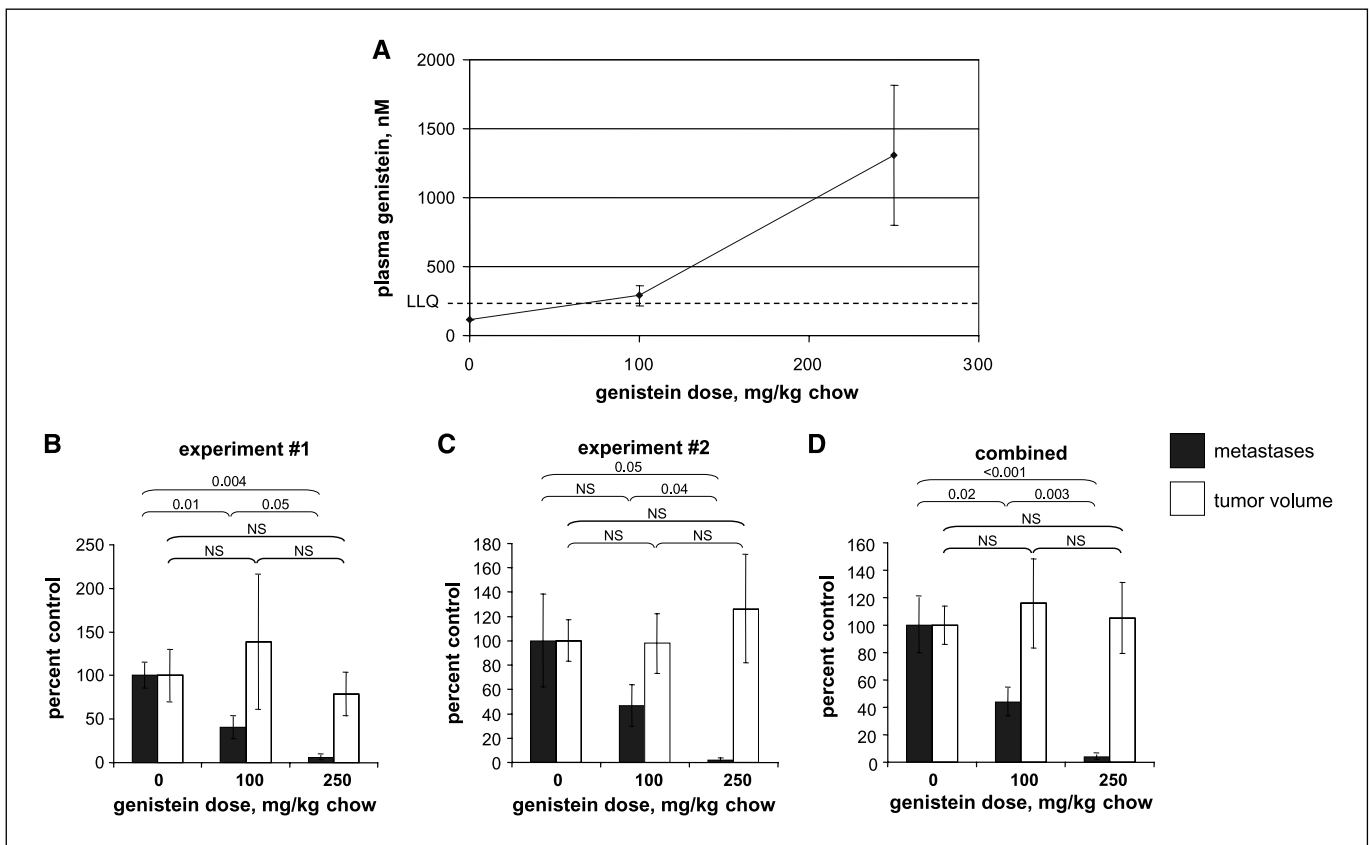
Figure 2. Genistein inhibits human PCa metastasis. Mice were fed chow containing 0 (for controls), 100, or 250 mg genistein/kg chow, implanted 1 wk later with 10^6 GFP-PC3-M cells, and tissue was harvested after 4 wk. Two separate and identical experiments were performed at separate times, involving a total of 10 mice per treatment cohort × 3 cohorts = 30 mice. *A,* blood genistein levels increase in a dose-dependent fashion. *Points,* mean plasma concentration of genistein; *bars,* SE. *B-D,* the effect of genistein upon tumor growth and metastasis. *Columns,* mean percentage of lung micrometastases and tumor volume, relative to controls, for mice in experiment 1 (*B*), experiment 2 (*C*), and for both experiments combined (*D*); *bars,* SE. Numbers above the brackets denote *P* values (two-sided *t* test) for the two groups at either end of a bracket. NS, not significant (i.e., *P* > 0.05).

treated with 0, 100, or 250 mg genistein/kg chow implanted with 10^6 cells, and necropsy was performed after 4 weeks. In each of two separate identical experiments performed at different times, there were five mice per treatment cohort. Thus, 30 mice in total were involved for the two experiments combined. In experiment 1, one mouse in each cohort died postsurgery.

Plasma total genistein concentration was measured in each mouse (Fig. 2*A*). For 0, 100, and 250 mg cohorts, the mean ± SE genistein concentration was below the LLQ, 290 ± 72 and 1307 ± 507 nmol/L, respectively. The mean steady-state plasma concentration of genistein in soy-consuming Japanese men was reported by Adlercreutz et al. to be 276 nmol/L (25). The mean peak plasma concentration in an older cohort of American men with PCa, after prospective oral dosing with ∼2× dietary amounts of soy-derived genistein, was shown by us to be 5,100 nmol/L (32). Thus, the current study attains blood concentrations which emulate those seen in both epidemiologic and prospective-based human studies.

In experiment 1, the mean ± SE percentage of control lung metastases was 40 ± 11% and 6 ± 2% for the 100 and 250 mg cohorts, respectively, Fig. 2*B* (ANOVA *P* = 0.0001). When compared with control, the decrease was statistically significant (*t* test *P* ≤ 0.05) for both the 100-mg and 250-mg cohorts. When compared with the 100-mg cohort, the additional decrease in the 250-mg

cohort was also statistically significant. In contrast to the pronounced antimetastatic effect of genistein, tumor volume was not significantly affected by genistein (ANOVA *P* = 0.66).

In experiment 2 (Fig. 2*C*), lung metastasis were 47 ± 15% and 2 ± 2% of control values for the 100-mg and 250-mg cohorts, respectively (ANOVA *P* = 0.0064). Compared with control, decreases in lung metastases were statistically significant for the 250-mg cohort (*t* test *P* ≤ 0.05) but not for the 100-mg cohort. Compared with the 100-mg cohort, the additional decrease in the 250-mg cohort was statistically significant. Tumor volume was not significantly affected by genistein (ANOVA *P* = 0.47).

Given the identical nature of experiments 1 and 2, we performed a combined analysis. Treatment with 100 and 250 mg genistein/kg chow significantly decreased metastases to 44 ± 9% and 4 ± 1% of control mice, respectively (ANOVA *P* < 0.0001; Fig. 2*D*). The decrease was statistically significant (*t* test *P* ≤ 0.05) for both the 100-mg and 250-mg cohorts when compared with control and for the 250-mg cohort when compared with the 100-mg cohort. Genistein had no significant effect upon tumor volume (ANOVA *P* = 0.92). Note that all mice in all cohorts had macroscopic lymph node metastases, and there was no difference in the weight of lymph nodes between the cohorts (data not shown).

Genistein induces PCa cell flattening *in vivo*. The above findings show that genistein inhibits PCa metastasis. Cell

detachment represents an initial step in the metastatic cascade (3, 5). Genistein inhibits PCa cell detachment *in vitro* (6, 7). We therefore investigated whether genistein could inhibit PCa cell detachment *in vivo*. Cell morphology reflects the attachment status of cells. Consequently, changes in cell morphology are used to measure changes in cell adhesion (39). We have previously shown that genistein-mediated increases in PCa cell attachment are associated with cell flattening *in vitro*, in a time-dependent and concentration-dependent fashion (6). The morphology of whole cells residing within intact solid organ tissue cannot be accurately quantitated. However, changes in cell morphology induce changes in nuclear morphology, and the latter can readily be assessed by quantitative image analysis in cells within tissue, including prostate (40, 41). For genistein, in particular, we have shown that its induction of cell flattening is associated with nuclear flattening (6).

As our prior assessment of *in vitro* morphology was qualitative, we first quantitated effects of genistein upon morphology *in vitro*. PC3-M cells were treated with 1 to 10,000 nmol/L genistein (0 nmol/L for controls) for 3 or 7 days, and cell and nuclear morphology were quantitated. As can be seen in Fig. 3A, genistein increased cell length (ANOVA P = 0.2 and 0.01 for 3 and 7 days, respectively) and cell area (0.2 and 0.01), as well as nuclear length (0.0007 and 0.0003) and nuclear area (<0.0001 and <0.0001), in a time-dependent and concentration-dependent fashion. The effects of genistein differed from control in a significant (t test $P \leq 0.05$) and consistent manner at lower concentrations after 7 days, compared with 3 days, for all variables evaluated. In addition, the magnitude of the change was greater after 7 days compared with 3 days. Importantly, changes in nuclear morphology mirrored those at the whole-cell level, particularly for the 7-day cohort. From representative cells treated with 1,000 nmol/L genistein × 7 days (Fig. 3B), it can be seen that the ability of genistein to induce cell and nuclear flattening are readily apparent visually.

The effects of genistein upon PCa cell nuclear morphometry *in vivo* was next evaluated. The morphometric variables which provide a measure of nuclear flattening are area, compactness, feret X, and feret Y; compactness = (perimeter)^2 / [4π (area)]. Maximum compactness is reflected by a value of 1, and is seen with a perfect circle. Perturbations of the circular shape, such as those induced by cell stretching, are reflected by an increase in the value of the compactness number. Ferets X and Y are derived by constructing the smallest box around a nucleus that will completely encompass that nucleus. The length and width of that box constitute ferets X and Y, respectively.

Metastatic lymph node tissue and primary tumor from the prostate were evaluated, and GFP-PC3-M cell morphology was compared between five control mice and five mice treated with
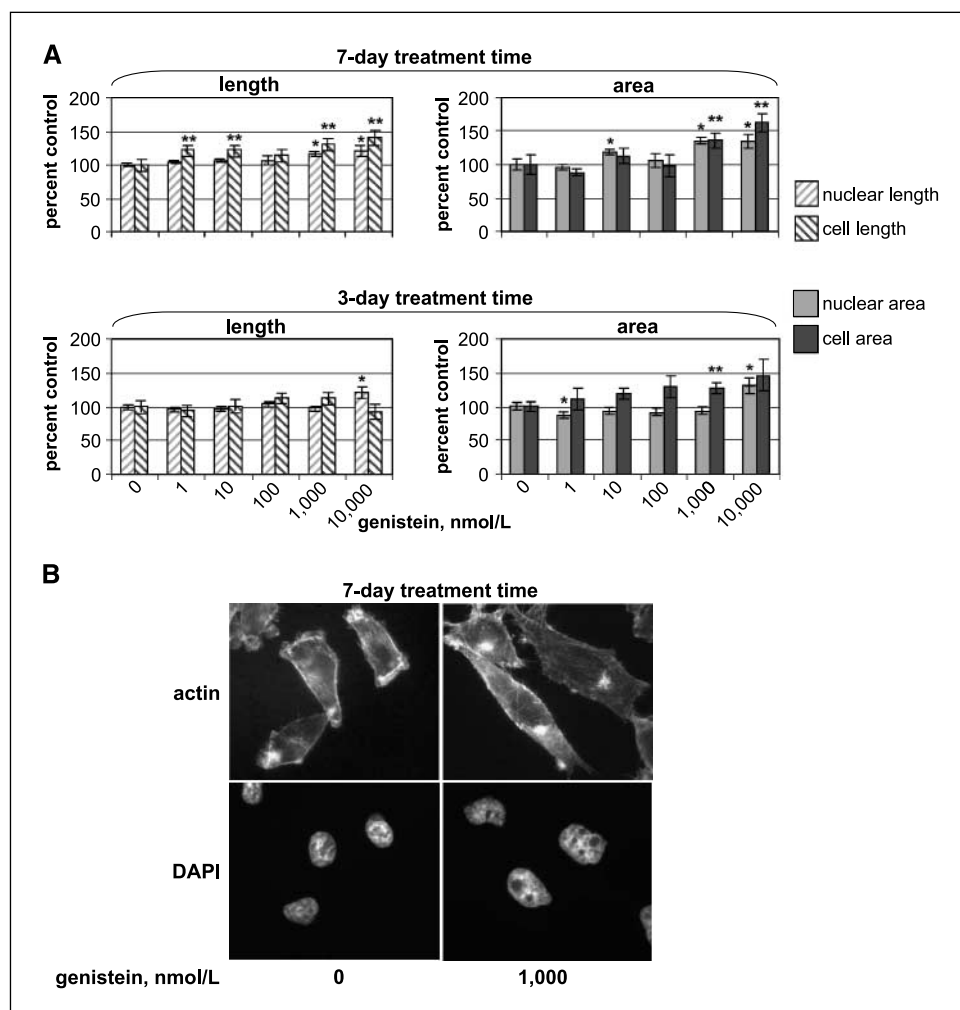
Figure 3. Genistein induces cell and nuclear flattening *in vitro*. PC3-M cells were treated with the indicated concentrations of genistein for either 3 or 7 d and then stained for filamentous actin (for whole cell imaging) or with DAPI (for nuclear imaging). *A,* the area and length of whole cells and their nuclei were then determined, as described in Materials and Methods; *columns,* mean (n = 10) percentage of control cells; *bars,* SE. Results are from a single experiment, with similar findings seen in multiple separate experiments. * and **, differences between cell and nuclear parameters, respectively, for $P \leq 0.05$ (two-sided t test). *B,* representative immunofluorescent photomicrographs of whole cells (actin) and their nuclei (DAPI) after treatment with 1,000 nmol/L genistein × 7 d are depicted; control cells were not treated.

A

Cell morphology of PC3-M cells in mice after treatment with genistein

| | primary tumor in prostate gland | | | | | | | |
| | area | | compactness | | feret X | | feret Y | |
treatment	mean	SE	mean	SE	mean	SE	mean	SE
control	120.44	2.27	1.57	0.01	12.82	0.15	13.17	0.14
genistein	121.26	1.83	1.6	0.01	13.2	0.13	13.13	0.13
P-value*	0.78		0.13		0.05		0.83	
percent increase	0.68		1.91		2.96		(-0.70)	

| | lymph node metastasis | | | | | | | |
| | area | | compactness | | feret X | | feret Y | |
treatment	mean	SE	mean	SE	mean	SE	mean	SE
control	87.27	1.5	1.41	0.03	11.11	0.11	10.71	0.11
genistein	104.3	1.79	1.46	0.01	12.12	0.12	11.73	0.12
P-value*	<0.01		<0.01		<0.01		<0.01	
percent increase	19.51		3.55		9.09		9.52	

*2 sided t test

B

control   genistein

Figure 4. Genistein alters human PCa cell nuclear morphology *in vivo*. *A,* nuclear morphometric analysis was performed on GFP-PC3-M cells present within primary tumor and lymph node tissue from five control mice and five mice treated with 250 mg genistein/kg chow, as described in Materials and Methods. *B,* representative photomicrographs of Feulgen-stained lymph node tissue (400×). Open and closed arrows indicate representative lymphocytes and GFP-PC3-M cells, respectively.
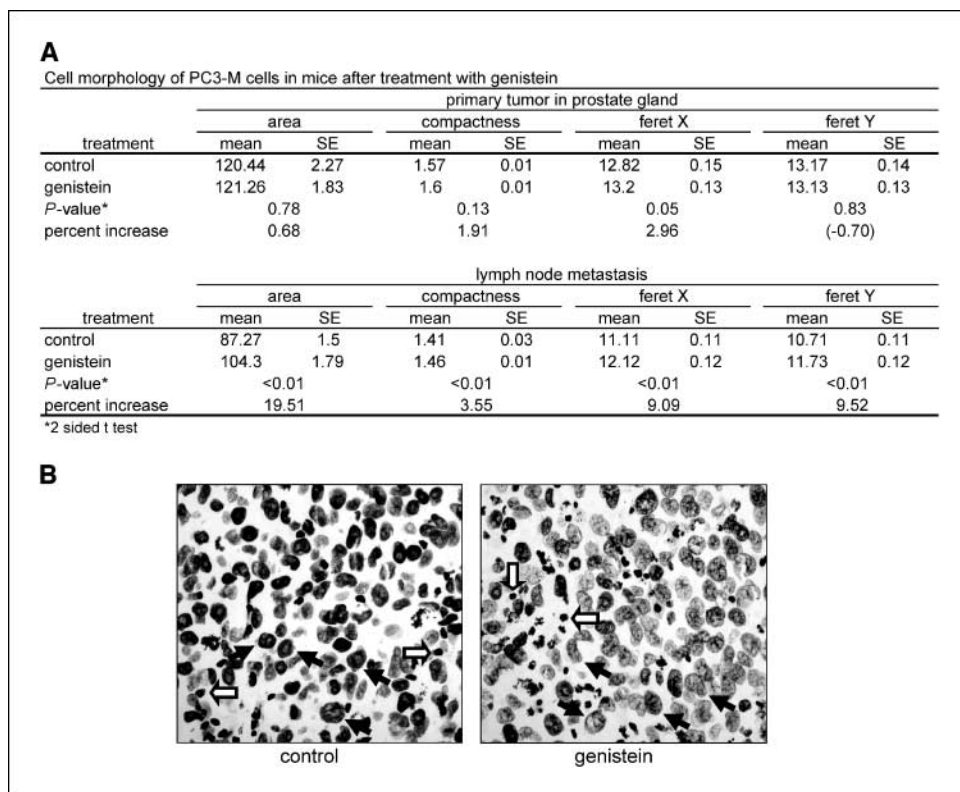
250 mg genistein/kg chow. The resultant nuclear morphometric variables are depicted in Fig. 4A. They indicate that genistein-induced nuclear flattening. Specifically, genistein induced statistically significant (t test $P \leq 0.05$) changes in the following variables: (*a*) increase in feret X in both primary tumor and lymph node, (*b*) increase in area and feret Y in lymph node, and (*c*) decrease in nuclear compactness (i.e., increase in the value of the nuclear compactness number) in lymph node. Furthermore, there was a trend toward an increase in the nuclear compactness number in primary tumor with genistein ($P = 0.13$).

Overall, both the magnitude and the statistical significance of genistein-induced nuclear flattening were greater in lymph node tissue than in primary tumor. These changes in the lymph node can be visually appreciated (Fig. 4B). In control tissue, GFP-PC3-M cell nuclei (solid arrows) tended to be rounded and dense. However, in genistein-treated tissue, cell nuclei tended to be less rounded, to exhibit less intense staining with increased granularity, and to be more spread out. The intensity of staining and morphology of lymphocytes (open arrows) was similar between the two tissues, thus providing a control.

Genistein increases expression, but not activation, of promotility proteins. Through a series of prior *in vitro* investigations, we have identified proteins which regulate PCa cell detachment and invasion and have shown that genistein inhibits their activation (7–9, 15, 16). Together, these studies implicate genistein-mediated inhibition of phosphorylation of FAK and of both p38 MAPK and HSP27 in genistein-mediated inhibition of cell detachment and invasion, respectively.

To evaluate *in vivo* effect of genistein upon these proteins, their level of expression was first measured in prostate tumor–derived protein by Western blot. By histomorphometry, >95% of tumor-associated cells were GFP-PC3-M. We have previously shown that

when measuring phosphorylated proteins, minimization of exposure to high intrinsic levels of prostate acid phosphatase is critical (17). For current study, experience has shown[5] that it is optimal to split the protein extract from a given mouse: use one half to exclusively measure total protein and use the other half to exclusively measure phosphorylated protein. This was done for five control mice and five mice treated with 250 mg genistein/kg chow.

Interestingly, genistein seemed to increase the expression of these "promotility" proteins (Fig. 5). Specifically, increases in FAK by 53% ($P = 0.04$) and p38 MAPK by 31% (<0.001) were significant, whereas the 16% increase in HSP27 represented a trend (0.07). Because genistein inhibits the promotility action of these proteins by blocking phosphorylation on residues which can be recognized by phosphorylation-specific antibodies (8, 15, 16), we next measured the ratio of phosphorylated protein to total protein (Fig. 5B). Importantly, this ratio was not increased by genistein and, in fact, seemed to be decreasing. Specifically, decreases in this ratio by 23% for p38 MAPK (one-sided t test $P = 0.03$) and by 12% for HSP27 (0.05) were significant, whereas the 12% decrease observed for FAK was not significant ($P = 0.23$). As we had previously shown that genistein decreased the phosphorylation of these proteins, we used a one-sided t test.

Discussion

We show for the first time that dietary genistein inhibits PCa metastasis. If genistein was in fact an active PCa antimotility drug in man, it would be expected that it should be effective in a variety

---

of relevant preclinical model systems. In this regard, it is important to note that antimetastatic efficacy of genistein in mice in the current study is consistent with our prior cell-based investigations which show that genistein inhibits initial steps in the metastatic cascade, namely, cell detachment and cell invasion (6–9). Epidemiologic findings further support the notion that genistein may be active in man. A number of studies associate dietary consumption of genistein with a lower mortality from PCa, and of particular interest, some suggest that there may be little effect upon the incidence of organ-confined PCa (26–29). The clinical relevance of genistein-mediated inhibition of PCa metastasis in the current study is also supported by the fact that efficacy was observed at genistein concentrations in the blood observed in man. The blood concentrations attained in mice in the current study correspond to those measured in men in epidemiologic dietary studies (25), as well as those measured by us and others (32, 42) in men with PCa after prospective dosing. The concentration of genistein is a critical factor when considering mechanism. This is because many mechanisms have been linked to genistein, but most require concentrations >2 logs above those attained in the blood after dietary intake (43, 44).

It was also shown for the first time that genistein induces flattening of cell nuclei *in vivo*, a measure of increased cell attachment. This represents a second measure of antimetastatic action, independent from the actual measure of metastases. However, given that cell detachment is an initial step in the metastatic cascade, a causal linkage is implicated. The current *in vivo* effects represent an extension of prior *in vitro* work, wherein genistein-mediated increase in PCa cell adhesion was associated with cell and nuclear flattening in several human PCa cell lines (6). Because it is not possible to accurately quantitate prostate cell morphology in intact tissue, nuclear morphology is routinely

measured (40, 41), as was done in the current study. As our prior *in vitro* analysis of cell and nuclear morphology was qualitative, it was important that we extended those findings in the current study by quantitatively evaluating effects *in vitro*. In this manner, we show that genistein-mediated effects upon nuclear morphology mirror cellular effects.

Interestingly, both the magnitude and the statistical significance of genistein-induced nuclear flattening were greater in lymph node tissue than in primary tumor. Although additional studies are necessary to elucidate the etiology of this observation, it likely relates to the fact that cells interact with different extracellular environments differently (in this case, the lymph node versus the prostate gland environment), as put forth in the "seed and soil" hypothesis (45). This notion is further supported in the current study by noting that differences in morphology exist between PCa cells in the prostate versus those in the lymph node, even within untreated mice (see Fig. 4A).

It was surprising to find that genistein increased the expression of "promotility" proteins. In particular, total levels of p38 MAPK and FAK were significantly increased, whereas the increase in total HSP27 represented a trend. It was thus important that we showed that genistein blocked the activation of these proteins *in vivo*. In fact, the levels of phosphorylated p38 MAPK and phosphorylated HSP27 were significantly decreased by genistein, whereas decrease of phosphorylated FAK in genistein only represented a trend. This is the first time genstein has been shown to inhibit activation of these proteins *in vivo*. Importantly, the current *in vivo* findings are consistent with our prior *in vitro* studies which show that genistein inhibits phosphorylation of FAK (15), p38 MAPK (8), and HSP27 (9), thereby inhibiting PCa cell detachment and invasion. Given that each of these proteins individually plays a role in regulating PCa cell motility, but together do so in a cooperative
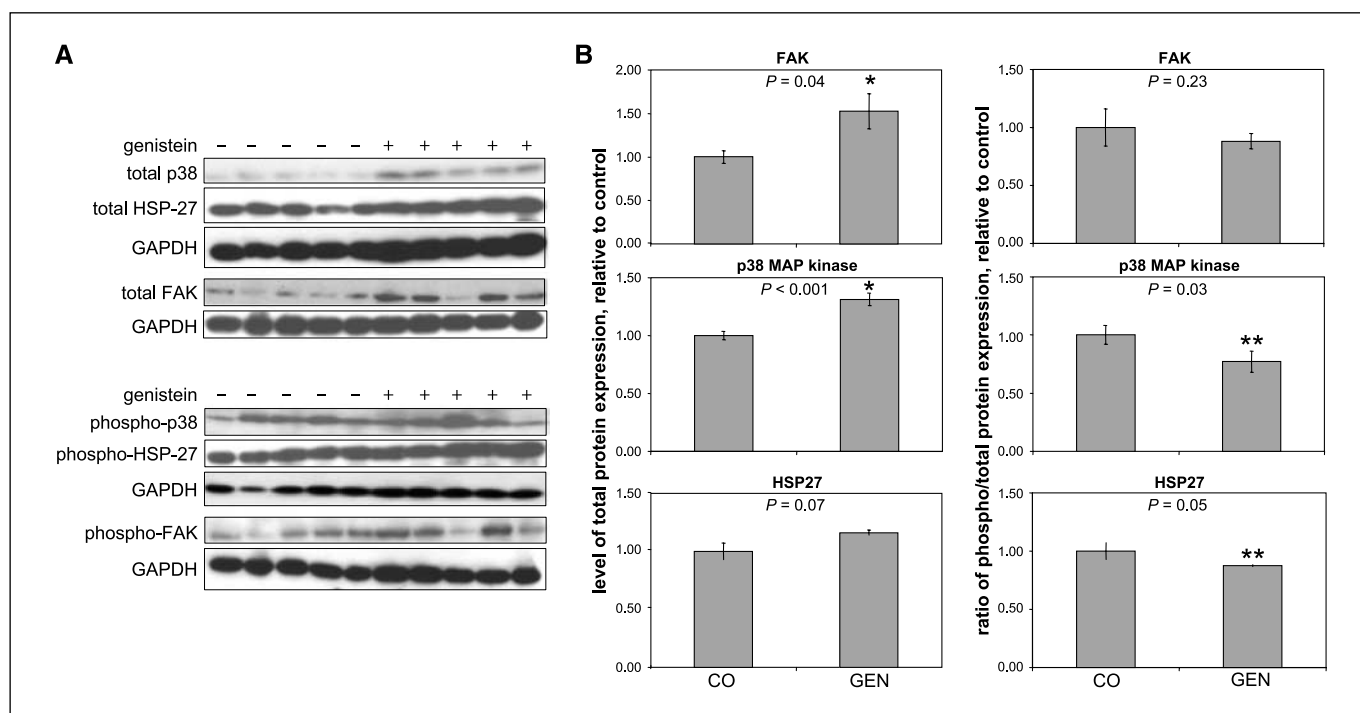
Figure 5. Genistein increases the expression of pro-motility proteins, but not their activation. *A,* protein was extracted from primary prostate tumors from five control mice and five mice treated with 250 mg genistein/kg chow, and Western blots were performed for total and phosphorylated FAK, p38 MAPK, and HSP27, as described in Materials and Methods. *B,* the density of individual bands was determined. *Columns,* resultant mean ratio of total protein/GAPDH and phosphorylated protein/total protein depicted; *bars,* SE. Values which differ from control by two-sided and one-sided *t* test *P* values of ≤0.05 are denoted by * and **, respectively.

fashion, it was of further importance that we evaluated them at the same time in the same model system. This is because it allowed us to determine that genistein led to relatively general increases in promotility proteins while blocking their activation and blocking cell motility. Together, these findings support the notion that pharmacologic inhibition of cell motility may cause the cell to mount a compensatory response. As distinct cell types, by definition, have homeostatic regulatory processes, this finding is not surprising. These points should be carefully considered in the interpretation of molecular biomarkers of efficacy, typically used in the conduct of human cancer chemoprevention trials (46). A failure to consider this possibility may wrongly lead one to conclude that a given chemopreventive agent is inducing an "undesirable" molecular phenotype, when in fact it is actually inhibiting the process being targeted.

The novel model described in the current study is well suited for testing the effect of agents upon human PCa metastasis. Its salient characteristics relate to the facts that lung metastases can be readily quantified, do not saturate the destination organ, and develop in the relatively short time frame of 4 weeks. Furthermore, it is a robust model and uses established cells directly from culture. Other metastatic models of PCa require serial passage of cell lines through mice, or implantation of solid tumor fragments, and involve assay times in excess of 3 months. In addition, it provides macroscopic primary and metastatic tumor. This allows the conduct of mechanism-specific studies and the assessment of growth inhibitory effects.

Genistein has estrogenic activity, and thus, some have implicated it as a potential anti-PCa mechanism (43). Although estrogenic activity of genistein is in fact very weak (47), we felt it important to evaluate potential hormone-based effects and did so in prior studies. Specifically, PC3-M cells have been shown by us to lack estrogen receptors, are known to lack androgen receptors, and do not respond to either hormone (13, 15). We have also shown that estrogen does not alter genistein efficacy upon PC3-M cells (6, 15). While the current study neither proves nor refutes an estrogen-associated mechanism for genistein in PCa, given these prior findings, it is unlikely that estrogen plays a role in mediating genistein effects in the current system.

The development of lymph node metastases seemed to require at least 2 weeks but did not otherwise correlate with time nor with the number of implanted cells. This likely reflects the fact that some factors cannot be controlled, e.g., the effect of hydrostatic pressure, induced by the surgical procedure itself upon lymphatic flow. In support of this notion, others who have used lymph node metastasis as a primary measure report that genistein increases metastasis (48). Whereas this finding seems to be in contrast to ours, it in fact provides another measure of genistein's ability to increase PCa cell adhesion. Specifically, PCa cells suspended in lymphatic fluid would be expected to more readily attach to regional lymph nodes in the presence of genistein. In contrast to lymph node metastasis, the development of lung metastases in the current study was dependent upon both

time and cell number. A number of factors suggest that hematologic seeding during surgical implantation was not a driving factor for the development of lung metastases. All implantations were done under direct visualization to ensure the formation of a stable subcapsular bleb. Also, uncontrolled hematologic seeding would be expected to cause wide variations in metastasis, and the associated loss of cells into the circulation should correlate with decreased primary tumor volume. These were not observed. Finally, given that genistein increases PCa cell adhesion, increased hematologic seeding would be expected to result in an increase in the number of metastases, at least in a subset of mice. This too was not observed.

The current model does have inherent limitations. They relate to the microscopic nature of lung metastasis (a barrier to molecular analysis) and the rapid growth of primary tumor (limits the assay time to 4 weeks). Measurement of metastases by use of qPCR for GFP did not provide a linear quantitation of GFP containing PC3-M DNA. We have extensive experience in performing qPCR on limiting amounts of tissue in a variety of different systems and were surprised by this finding (33, 49, 50). It is possible that further technical refinement can overcome this limitation. Until that time, quantitation of lung micrometastases should be performed by histomorphometry. Finally, the current model only permits investigation of metastasis in lung and lymph node tissue. In the particular case of genistein, which acts to inhibit PCa cell detachment from the primary organ, there is no reason to believe that efficacy would be limited to a single distant organ, in this case, lung.

Collectively, our findings characterize a robust model of human PCa metastasis suitable for testing the efficacy of antimetastatic agents. In this model, dietary genistein was shown to decrease human PCa metastasis in a dose-dependent manner. Associated mechanistic studies implicate genistein-mediated inhibition of PCa cell detachment. They also indicate that cellular compensatory responses may in fact lead to increases in promotility proteins, but further suggest that genistein inhibits their activation. These *in vivo* findings corroborate *in vitro* studies, which together support the notion that genistein-mediated inhibition of PCa metastasis may be in part responsible for the lower mortality associated with dietary genistein consumption. A more definitive linkage between a genistein-mediated antimetastatic mechanism and epidemiologic findings will require a dedicated analysis of genistein effects upon human prostate cells in humans. We have completed a phase 1 trial of genistein in men with PCa (32) and have implemented a phase 2 trial designed to evaluate genistein antimotility effect upon PCa cells in man.

Acknowledgments

References

1. Jemal A, Siegel R, Ward E, Murray T, Xu J, Thun MJ. Cancer statistics, 2007. CA Cancer J Clin 2007;57: 43–66.
2. Carroll PR, Lee KL, Fuks ZY, Kantoff PW. Cancer of the Prostate. In: DeVita VT, Hellman S, Rosenberg SA, editors. CANCER: Principals and Practices of Oncology. New York: Lippincott-Raven; 2001. p. 1418–79.
3. Ruoslahti E. How cancer spreads. Sci Am 1996;275: 72–7.
4. Stetler-Stevenson WG, Yu AE. Proteases in invasion: matrix metalloproteinases. Semin Cancer Biol 2001;11: 143–52.
5. Woodhouse EC, Chuaqui RF, Liotta LA. General mechanisms of metastasis. Cancer 1997;80:1529–37.
6. Bergan R, Kyle E, Nguyen P, Trepel J, Ingui C, Neckers L. Genistein-stimulated adherence of prostate cancer

cells is associated with the binding of focal adhesion kinase to β-1-integrin. Clin Exp Metastasis 1996;14: 389–98.

7. Liu YU, Kyle E, Lieberman R, Crowell J, Kelloff G, Bergan RC. Focal adhesion kinase (FAK) phosphorylation is not required for genistein-induced FAK-b-1-integrin complex formation. Clin Exp Metastasis 2000;18:203–12.

8. Huang X, Chen S, Xu L, et al. Genistein inhibits p38 map kinase activation, matrix metalloproteinase type 2, and cell invasion in human prostate epithelial cells. Cancer Res 2005;65:3470–8.

9. Xu L, Bergan RC. Genistein inhibits MMP-2 activation and prostate cancer cell invasion by blocking TGF{β}-mediated activation of MAPKAPK2–27 pathway. Mol Pharmacol 2006;70:869–77.

10. Schaller MD, Borgman CA, Cobb BS, Vines RR, Reynolds AB, Parsons JT. pp125FAK a structurally distinctive protein-tyrosine kinase associated with focal adhesions. Proc Natl Acad Sci U S A 1992;89:5192–6.

11. Hanks SK, Calalb MB, Harper MC, Patel SK. Focal adhesion protein-tyrosine kinase phosphorylated in response to cell attachment to fibronectin. Proc Natl Acad Sci U S A 1992;89:8487–91.

12. Cobb BS, Schaller MD, Leu TH, Parsons JT. Stable association of pp60src and pp59fyn with the focal adhesion-associated protein tyrosine kinase, pp125FAK. Mol Cell Biol 1994;14:147–55.

13. Liu YQ, Kyle E, Patel S, et al. Prostate cancer chemoprevention agents exhibit selective activity against early stage prostate cancer cells. Prostate Cancer Prostatic Dis 2001;4:81–91.

14. Tremblay L, Hauck W, Aprikian AG, Begin LR, Chapdelaine A, Chevalier S. Focal adhesion kinase (pp125FAK) expression, activation and association with paxillin and p50CSK in human metastatic prostate carcinoma. Int J Cancer 1996;68:164–71.

15. Kyle E, Neckers L, Takimoto C, Curt G, Bergan R. Genistein-induced apoptosis of prostate cancer cells is preceded by a specific decrease in focal adhesion kinase activity. Mol Pharmacol 1997;51:193–200.

16. Xu L, Chen S, Bergan RC. MAPKAPK2 and HSP27 are downstream effectors of p38 MAP kinase-mediated matrix metalloproteinase type 2 activation and cell invasion in human prostate cancer. Oncogene 2006;25: 2987–98.

17. Hayes SA, Huang X, Kambhampati S, Platanias LC, Bergan RC. p38 MAP kinase modulates Smad-dependent changes in human prostate cell adhesion. Oncogene 2003;22:4841–50.

18. Liu Y, Jovanovic B, Pins M, Lee C, Bergan RC. Over expression of endoglin in human prostate cancer suppresses cell detachment, migration and invasion. Oncogene 2002;21:8272–81.

19. Craft CS, Romero D, Vary CPH, Bergan RC. Endoglin inhibits prostate cancer motility via activation of the ALK2-1 pathway. Oncogene 2007;26:7240–50.

20. Craft CS, Xu L, Romero D, Vary CPH, Bergan RC. Genistein induces phenotypic reversion of endoglin defi-ciency in human prostate cancer cells. Mol Pharmacol 2008;73:235–42.

21. Rocchi P, Beraldi E, Ettinger S, et al. Increased Hsp27 after androgen ablation facilitates androgen-independent progression in prostate cancer via signal transducers and activators of transcription 3-mediated suppression of apoptosis. Cancer Res 2005;65: 11083–93.

22. Rocchi P, So A, Kojima S, et al. Heat shock protein 27 increases after androgen ablation and plays a cytoprotective role in hormone-refractory prostate cancer. Cancer Res 2004;64:6595–602.

23. Cornford PA, Dodson AR, Parsons KF, et al. Heat shock protein expression independently predicts clinical outcome in prostate cancer. Cancer Res 2000;60: 7099–105.

24. Messina MJ, Persky V, Setchell KD, Barnes S. Soy intake and cancer risk: a review of the *in vitro* and *in vivo* data. Nutr Cancer 1994;21:113–31.

25. Adlercreutz H, Markkanen H, Watanabe S. Plasma concentrations of phyto-oestrogens in Japanese men. Lancet 1993;342:1209–10.

26. Adlercreutz H. Western diet and Western diseases: some hormonal and biochemical mechanisms and asso-caitions. Scand J Clin Lab Invest 1990;50 Suppl 201:3–23.

27. Shimizu H, Ross RK, Bernstein L, Yatani R, Henderson BE, Mack TM. Cancers of the prostate and breast among Japanese and white immigrants in Los Angeles County. Br J Cancer 1991;63:963–6.

28. Severson RK, Nomura AM, Grove JS, Stemmermann GN. A prospective study of demographics, diet, and prostate cancer among men of Japanese ancestry in Hawaii. Cancer Res 1989;49:1857–60.

29. Cook LS, Goldoft M, Schwartz SM, Weiss NS. Incidence of adenocarcinoma of the prostate in Asian immigrants to the United States and their descendants. J Urol 1999;161:152–5.

30. Simpson L, He X, Pins M, et al. Renal medullary carcinoma and ABL gene amplification. J. Urology 2005; 173:1883–8.

31. Bergan R, Hakim F, Schwartz GN, et al. Electro-poration of synthetic oligodeoxynucleotides: a novel technique for *ex vivo* bone marrow purging. Blood 1996; 88:731–41.

32. Takimoto CH, Glover K, Huang X, et al. Phase I pharmacokinetic and pharmacodynamic analysis of unconjugated soy isoflavones administered to individuals with cancer. Cancer Epidemiol Biomarkers Prev 2003;12:1213–21.

33. Kelley MJ, Glaser EM, Herdon JE, et al. Safety and efficacy of weekly oral oltipraz in chronic smokers. Cancer Epidemiol Biomarkers Prev 2005;14:892–9.

34. Venkataraman G, Ananthanarayanan V, Paner GP, et al. Morphometric sum optical density as a surrogate marker for ploidy status in prostate cancer: an analysis in 180 biopsies using logistic regression and binary recursive partitioning. Virchows Arch 2006;449: 302–7.

35. Bacus JW, Boone CW, Bacus JV, et al. Image morphometric nuclear grading of intraepithelial neoplastic lesions with applications to cancer chemoprevention trials. Cancer Epidemiol Biomarkers Prev 1999;8:1087–94.

36. Lakshman M, Subramaniam V, Jothy S. CD44 negatively regulates apoptosis in murine colonic epithelium via the mitochondrial pathway. Exp Mol Pathol 2004;76:196–204.

37. Lakshman M, Subramaniam V, Wong S, Jothy S. CD44 promotes resistance to apoptosis in murine colonic epithelium. J Cell Physiol 2005;203:583–8.

38. Uzgare AR, Isaacs JT. Prostate cancer: potential targets of anti-proliferative and apoptotic signaling pathways. Int J Biochem Cell Biol 2005;37:707–14.

39. Humphries MJ. Cell adhesion assays. Mol Biotechnol 2001;18:57–61.

40. Bartels PH, Montironi RM, Bostwick D, et al. Karyometry of secretory cell nuclei in high-grade PIN lesions. Prostate 2001;48:144–55.

41. Veltri RW, Partin AW, Miller MC. Quantitative nuclear grade (QNG): a new image analysis-based biomarker of clinically relevant nuclear structure alterations. J Cell Biochem 2000;Suppl 35:151–7.

42. Fischer L, Mahoney C, Jeffcoat AR, et al. Clinical characteristics and pharmacokinetics of purified soy isoflavones: multiple-dose administration to men with prostate neoplasia. Nutr Cancer 2004;48:160–70.

43. Clinical development plan: genistein. J Cell Biochem Suppl 1996;26:114–126.

44. Nabhan C, Bergan R. Chemoprevention in prostate cancer. In: Bergan RC, editor. Cancer Chemoprevention. Boston: Kluwer Academic Publishers; 2001. p. 103–36.

45. Fidler IJ. The pathogenesis of cancer metastasis: the 'seed and soil' hypothesis revisited. Nat Rev Cancer 2003; 3:453–8.

46. Kosmeder JW, Pezzuto JM. Intermediate Biomarkers. In: Bergan RC, editors. Cancer Chemoprevention. Boston: Kluwer Academic Publishers; 2001. p. 31–62.

47. Matsumura A, Ghosh A, Pope GS, Darbre PD. Comparative study of oestrogenic properties of eight phytoestrogens in MCF7 human breast cancer cells. J Steroid Biochem Mol Biol 2005;94:431–43.

48. Wang Y, Raffoul JJ, Che M, et al. Prostate cancer treatment is enhanced by genistein *in vitro* and *in vivo* in a syngeneic orthotopic tumor model. Radiat Res 2006; 166:73–80.

49. Ding Y, Xu L, Chen S, et al. Characterization of a method for profiling gene expression in cells recovered from intact human prostate tissue using RNA linear amplification. Prostate Cancer Prostatic Dis 2006;9: 379–91.

50. Schwartz GN, Liu YQ, Tisdale J, et al. Growth inhibition of chronic myelogenous leukemia cells by ODN-1, an aptameric inhibitor of p210bcr-abl tyrosine kinase activity. Antisense Nucleic Acid Drug Dev 1998;8: 329–39.